Miscible viscous fingering in microgravity

A. Aubertin, G. Gauthier, J. Martin, D. Salin, and L. Talon
Université Paris–Sud, Université Pierre et Marie Curie–Paris 6, CNRS, F-91405, Laboratoire FAST, Bat. 502, Campus Univ., Orsay F-91405, France

(Received 4 February 2009; accepted 17 April 2009; published online 27 May 2009)

To address the issue of miscible viscous fingering instability in buoyancy free conditions, experiments have been performed under microgravity conditions in parabolic flights. A Hele-Shaw cell, two parallel plates separated by a small gap, has been used with two miscible fluids of viscosity ratio 100 (the injected fluid is the less viscous). The influence of the initial thickness of the pseudointerface between the two fluids has been studied, using flow rates large enough to prevent further mixing during displacement. The selected wavelength, measured on the observed fingering pattern, does not depend on the initial front thickness: It is around three times the gap of the cell, i.e., significantly lower than the value of five, observed on earth. However, the initial thickness does control the displacement length required for the instability to occur. Our results are in reasonable agreement with existing and new numerical simulations. © *2009 American Institute of Physics*.
[DOI: 10.1063/1.3134662]

I. INTRODUCTION

Viscous fingering refers to the instability occurring when a less viscous fluid displaces a more viscous one. The origin of the instability was studied in Hele-Shaw cells (two parallel plates separated by a small gap) for immiscible displacement in pioneering works by Saffman and Taylor,[1] and for miscible displacement by Hill[2] and Wooding.[3] A number of works has been since devoted to the specific case of porous media, (e.g., see reviews[4,5] and a more recent analysis[6]) and to the more general issue of the stability of miscible displacements in confined medium.[5,7–11] We note that in such displacements, any mismatch of the fluids densities introduces a long-wave gravity effect, which can be stabilizing or destabilizing, depending on the direction of the displacement and the densities of the two fluids. A crucial difference between viscous fingering in porous media (obeying Darcy's law) and in Hele-Shaw cell, comes from the length scale (the gap thickness) introduced by the confinement in the latter case. In a homogeneous porous medium,[12] Tan and Homsy predicted the finger size to scale with the dispersivity (the only available scaling length) for a sharp initial interface, and to decrease for increasing interface thickness. We note that the latter prediction may also apply to Hele-Shaw cells, for the case of thick interfaces (significantly thicker than the gap of the cell, e), for which Darcy's law may remain valid during the fingering process, or in the low Peclet number regime,[13] i.e., for flow rates low enough for molecular diffusion to mix efficiently the two fluids across the gap. On the contrary, for thin initial interfaces and for moderate to large Peclet number displacements, the pattern observed in a Hele-Shaw cell consists, in a first step, in a tongue of the less viscous fluid developing symmetrically in the middle of the gap with roughly a half gap thickness.[14,10] In the presence of stabilizing buoyancy, a flow rate threshold exists, above which viscous forces can overcome buoyancy ones, and a fingering instability of the tongue appears further on.[15,16] The resulting pattern consists of regular fingers spanning the width of the cell, with a spatial wavelength of nearly five times the gap thickness, obtained both in experiments[15] and in numerical simulations.[17] On another hand, the numerical stability analysis of the tongue developing in the absence of buoyancy, i.e., pure viscous fingering, predicts a value of nearly three times the gap thickness.[18] Hence, the buoyancy would increase the wavelength of the viscous instability, which is rather unexpected from a long-wave stabilizing effect. This indicates at least that the interplay between buoyancy and viscous phenomena is far from being trivial. The purpose of this paper is precisely to address experimentally the issue of pure miscible fingering in a Hele-Shaw cell. At first sight, avoiding buoyancy effects might be achieved by matching the densities of the two fluids, but in this case, controlled initial conditions on the pseudo interface would be nearly unobtainable: Experimentally, buoyancy may tremendously help to achieve initial conditions of flat pseudointerface, but should be removed at the onset of the flow if one wants to address pure miscible fingering. Such contradictory experimental requirements can be obtained in parabolic flights which provide successive phases of microgravity and of hypergravity (5/1000 and 2 times the earth gravity, respectively). We have carried out experiments of pure viscous fingering in such flights. An experimental protocol has been defined in order to get the most of the so-provided series of buoyant/unbuoyant sequences within the frame of the constraints of the flights. Accordingly, the experiments have been carried out with a fixed pair of miscible fluids, and different initial thicknesses of the pseudo interface. We present the study of the influence of this initial thickness on the pure viscous fingering instability characteristics, namely, the wavelength of the fingers and the onset of the instability.

II. EXPERIMENTS

The Hele-Shaw cell consists of two parallel glass plates of length $l=800$ mm and width $w=100$ mm (see Fig. 1), separated by a gap thickness $e=1$ mm. The x, y, and z axes are defined along the length, the width, and the thickness directions, respectively. The cell is "held vertically" along

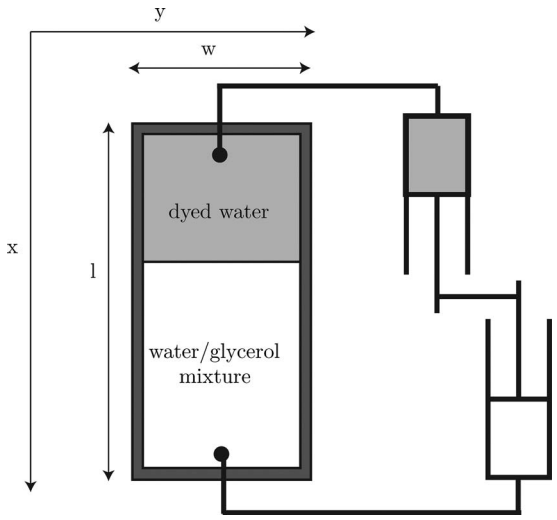

FIG. 1. Sketch of the experimental setup. The less viscous fluid is injected (withdrawn) from the top whereas the thicker fluid is withdrawn (injected) from the bottom during injection (restoring) phase, under microgravity (hypergravity).

the x axis in the sense that when existing, the gravity aligns with the x axis. Therefore, the x axis will be considered as oriented from the top to the bottom of the cell, and so will be the flow imposed in the microgravity phases. The fixed pair of fluids is composed of blue dyed water (viscosity $\mu_w = 10^{-3}$ Pa s and density $\rho_w = 1000$ kg/m^3) and transparent water-glycerol mixture (viscosity $\mu_m = 100.10^{-3}$ Pa s and density $\rho = 1200$ kg/m^3). The fixed destabilizing flow rate sets the average flow velocity to the value $U_0 = 15$ mm/s. Such a velocity is large enough to prevent diffusive mixing between the fluids during displacement (Péclet number $\mathrm{Pe} = U_0 e / D_m \sim 10^4$, D_m molecular diffusion coefficient) and low enough to get a laminar base flow (Reynolds number $\mathrm{Re} = \rho_w U_0 e / \mu_w \sim 15$). The cell, held vertically, was filled just before the flight. The heavy fluid (water-glycerol mixture) was first injected from the bottom of the cell, and subsequently, the lighter one was injected slowly from the top, in order to minimize the mixing of the fluids. The stabilizing effect of buoyancy achieved the initial condition of a "flat" horizontal pseudo interface, with an initial thickness equal to a few gap thickness.

The experiment was recorded using a video camera. The transmitted light intensity gives, after calibration, a quantitative measurement of the concentration of the dyed less viscous fluid,[10] averaged over the gap of the cell. The so-obtained concentration map $C(x,y)$ does not depend on y in the initial state [Fig. 2(a)], and allows the measurement of the pseudo interface thickness δ by fitting the initial concentration profile, displayed in Fig. 2(b), with an error function $[C = \mathrm{erf}((x-a)/\delta)]$.

Experiments were performed during the 54th CNES parabolic flight campaign in the Airbus A300 Zero-G. The parabolic flights provided 32 successive, 20 s long, phases of "microgravity" ($\|\vec{g}\| = 0 \pm 0.05$ m/s^2), followed by a few seconds long "hypergravity" phases ($\|\vec{g}\| = 19.6$ m/s^2), and a few minutes long phases of "normal" earth gravity. For each parabola, our experimental sequence was the following: During 6 s, the lighter fluid was first injected from the "top" while the heavier one was withdrawn from the bottom (phase of "pure viscous fingering experiment"). Then the flow was stopped for 3 s, and reversed, at the same rate, for 6 s, and stopped again, until the next parabola. With this protocol, the net mean displacement of the interface during the sequence is zero, and with the help of the gravity, a flat interface is restored before the next parabola [Fig. 2(a)]. However, due to the mixing induced by the viscous fingering instability, the so-restored horizontal interface gets thicker and thicker after each parabola so that the influence of δ on the viscous fingering can be addressed, using this protocol.

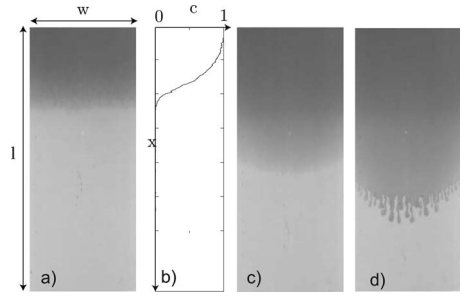

FIG. 2. (a) Picture of the initial interface between the two fluids. (b) Corresponding gap-averaged concentration profile. (c) Picture of the interface just before fingering. (d) Picture of the developed fingering pattern.

Figures 2(c) and 2(d) display typical pictures of the pattern observed just before fingering (c) and after fingering (d). The wavelength, λ, of the fingers was measured on Fig. 2(d) and on similar pictures, just after the digitation onset. Note that the pseudointerface exhibits a small overall curvature, not observed on earth, most likely due to a residual radial effect of injecting from one point. For that reason, λ, as well as the concentration profiles $C(x)$, were measured in the central region of the cell. More precisely, the measured values for λ and Δλ were given by the average and the standard deviation of the distance between fingers.

The so-obtained wavelengths, λ, collected during the different parabola, are plotted versus the initial front thickness, δ, on Fig. 3: The measured values merge on a constant value $\lambda = (3.2 \pm 0.5)e$ (solid line on the figure), significantly smaller than the experimental value obtained with stabilizing

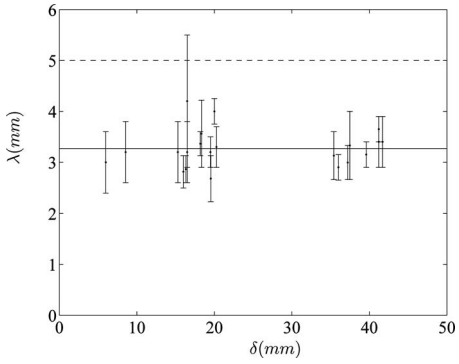

FIG. 3. Wavelength of the fingering pattern versus the initial interface thickness δ. The lines correspond to the wavelength obtained for a thin interface $\delta \simeq 0$, in experiments with buoyancy (Ref. 10) (dashed line), and in numerical simulations without buoyancy (Ref. 18) (solid line).

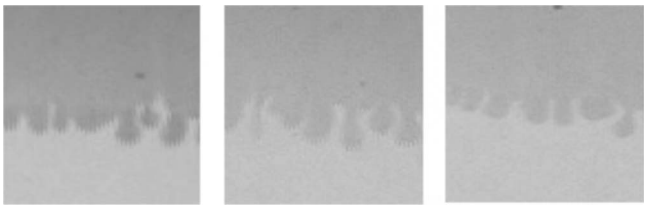

FIG. 4. Fingering patterns observed for various initial interface thicknesses (from left, to right: $\delta \simeq 8e, 15e, 19e$), at front locations $l_t \simeq 25e, 41e, 57e$, respectively.

buoyancy,[15] $\lambda_{\text{buoyant}} = (5.2 \pm 0.5)e$ (dashed line on the figure). We note that even for an initial interface as thick as $\delta \simeq 40e$, no dependence on δ is observed, which disagrees with predictions of Tan and Homsy.[12] This indicates that Darcy's law, used in Ref. 12, does not apply to the gap-averaged velocity, in our experiments. Actually, our measured wavelength rather compares with the value 3.17 obtained by Goyal and Meiburg[18] in the absence of buoyancy. We recall that these authors performed a numerical linear stability analysis of the two-dimensional (2D) tongue which, for a sharp initial interface, is supposed to develop in the gap before the onset of the fingering instability. Although no initial thin interface has been tested in our experiments (the interface thickness was at least $\delta \simeq 5e$), we note that this "tongue approach" was first used, successfully, in the case of buoyancy to handle initial interface thicknesses comparable to our lower ones.[15,10,16] More puzzling indeed is that the prediction for λ, obtained with this approach, still holds for $\delta \simeq 40e$. More generally, the fingering patterns obtained in the range $5e < \delta < 40e$ were very similar (see Fig. 4), but were observed later and later, as δ was increased.

To quantify this last feature, we have measured the traveled distance, l_t, of the leading edge of the front (given by the tip location, l_t), at the onset of the fingering [i.e., on pictures corresponding to Fig. 2(c)]. The so-obtained values, denoted by l_d, are displayed on Fig. 5. A linear dependence of l_d with δ is obtained over the entire range of initial interface thickness: $l_d \approx 3\delta$. We note that l_d represents the displacement during which the interface remains invariant along the width of the cell, while being stretched along the flow

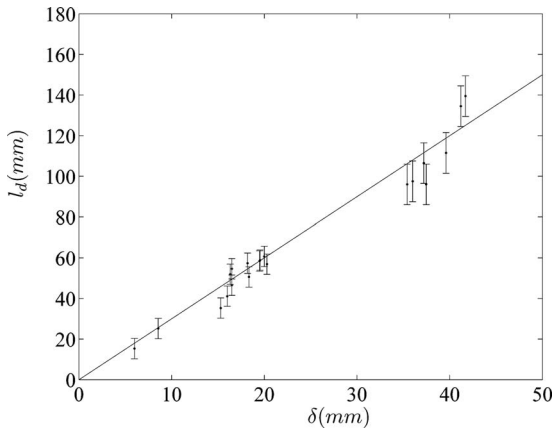

FIG. 5. Front displacement at the onset of the 3D instability, l_d, vs the initial interface thickness, δ. The solid line is the linear fit to the data: $l_d = 3\delta$.

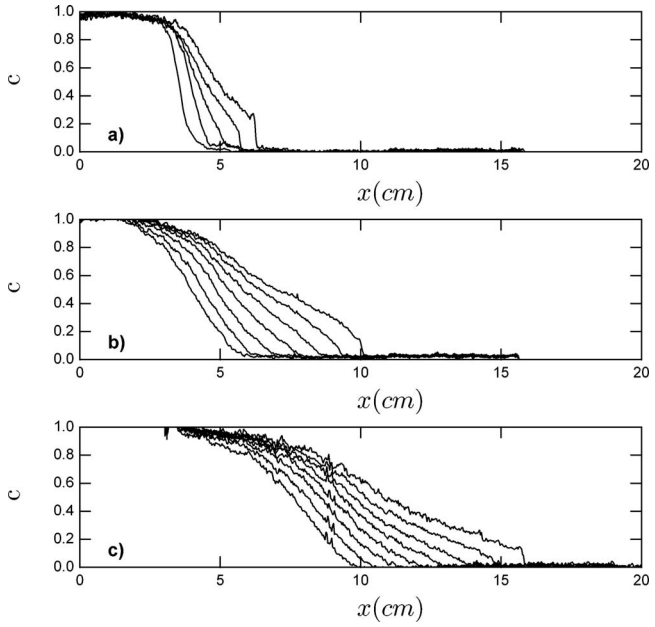

FIG. 6. Gap-averaged concentration profiles, $C(x)$, along the streamwise x direction (direction of the flow), measured in the middle of the cell, at different times. In each series, the first and last profiles are obtained at the onset of injection and fingering, respectively. The subplots correspond to three different parabola, i.e., three initial interface thicknesses δ: (a) first parabola, $\delta = 6e$, (b) sixth parabola $\delta = 16e$, and (c) sixteenth $\delta = 24e$. The time interval between two profiles is 0.2 s for (a) and (b), and 0.4 s for (c).

(2D regime). An insight into the deformation of the interface in the gap of the cell is given by the profiles of the gap-averaged concentration $C(x)$.

Figures 6(a)–6(c) display such profiles measured at regular time intervals, from the beginning of the injection up to the onset of the three-dimensional (3D) fingering for different δ.

During the displacement starting from a well mixed initial state, the profiles spread rather linearly in time, with the exception of their leading edge. The latter sharpens in time and becomes almost steplike when the 3D fingering transition occurs. This type of behavior has been already observed in the buoyant case by Lajeunesse *et al.*[10,15] and has been understood as the development of a tongue of less viscous fluid in the middle of the gap, as shown in Fig. 7. Moreover the detailed shape of these tonguelike profiles has been completely interpreted in the framework of kinematic waves.[10,15,19] The normalized tongue thickness predicted by[19] in the present case, for $M = 100$, has been compared to the heights of the concentration steps measured just before the instability. The predicted value $C = 0.22$ falls in the higher

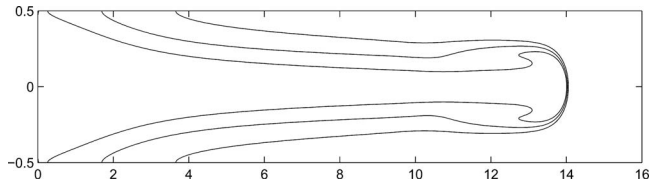

FIG. 7. 2D numerical simulations. Isoconcentration contours ($c = 0.1, 0.5, 0.9$) of the displacement of a front in the gap of a Hele-Shaw cell, for an initial thickness $\delta = 2\ e$.

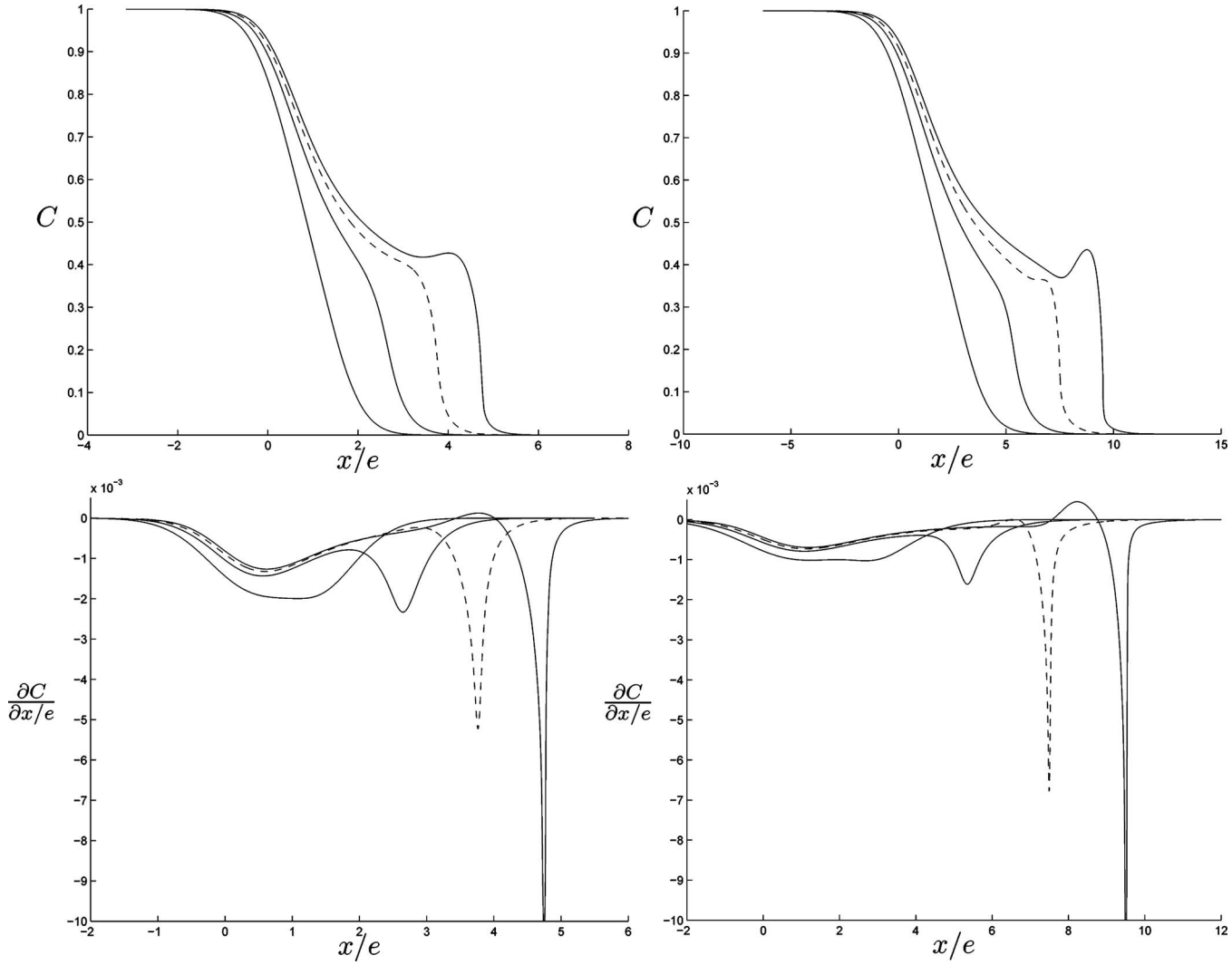

FIG. 8. 2D numerical simulations. Top: concentration profiles for two different initial thicknesses (left: $\delta=e$, right: $\delta=2e$), corresponding to four normalized front locations ($l_t/\delta=1,2,3,4$). The dashed line curves correspond to the front location $l_t=l_d$ at which the fingering occurs in the experiments. Bottom: corresponding concentration gradient.

range of our dispersed measurements $C=0.17\pm0.05$. However, we have to point out that the kinematic wave model assumes a flux function fixed by the concentration C. In the present case, this would require that the two fluids do not mix in the gap. This condition of a sharp pseudointerface is not fulfilled at the initial time of our displacements, although it is approached during the 2D prefingering regime. As a consequence, it has not been possible to analyze the time evolution of our concentration profiles with the kinetic wave approach. Alternatively, we performed 2D numerical simulations of the displacement in the gap.

III. SIMULATIONS

We used a numerical scheme of finite compact difference method similar to the one of Ref. 18 with a mesh of 3200×300 and with $\mathrm{Pe}=2000$. Because of computational time issue, our numerical study was restricted to initial front thicknesses $\delta\leq2.5e$. Figure 7 gives three isoconcentration contours of a typical 2D pattern obtained for $\delta=2e$. The simulation confirms the formation of a symmetric 2D tongue developing in the gap of the Hele-Shaw cell. Figure 7 demonstrates also the thinning of the pseudointerface, in particular at the leading edge of the tongue.

From the gap average of such concentration maps, one derives the concentration profiles $C(x)$. Figure 8 displays two sets of such profiles, obtained for two different initial front thicknesses (top left: $\delta=e$, top right: $\delta=2e$), with the corresponding derivatives $\partial\bar{C}/\partial x/e$ (bottom). We note that the characteristic features of the evolution of the profiles observed in experiments (Fig. 6) are recovered in simulations (top of Fig. 8). Moreover, the profiles (and derivatives) of Fig. 8, obtained for the same values of l_t/δ, look similar. This remark applies in particular for the profiles obtained at $l_t=l_d=3\delta$ (in dashed line on Fig. 8), which correspond to the onset of the $3D$ destabilization. Qualitatively, these profiles look like a "shock" structure (known to be unstable[1]), with the appearance of a steep leading part, followed by a low gradient part (i.e., an inflexion point with a slope approaching zero in the vicinity of $l_t=l_d=3\delta$).

To test more quantitatively the scaling of the evolution

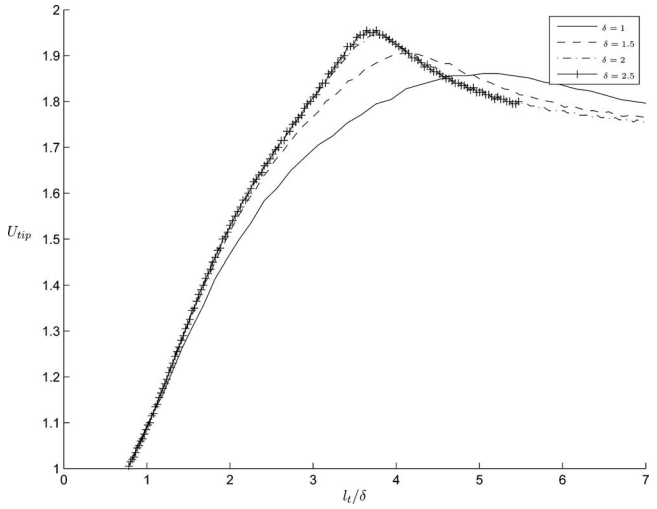

FIG. 9. Front velocity, U_{tip}, vs the normalized front location, l_t/δ, for different initial thicknesses δ. One can note that the velocity stabilizes for displacements larger than five times the initial thickness.

of the 2D regime, we plotted in Fig. 9 the evolution of the tip velocity, U_{tip}, with the normalized displacement, l_t/δ, for different initial δ. Even though some discrepancy is observed for initial thicknesses as small as $\delta=e$ and $\delta=1.5e$, the curves obtained for $\delta=2e$ and $\delta=2.5e$ collapse nearly perfectly. This again supports the contention that, for the range of δ addressed in the experiments, the 2D unstable base state, reached at $l_t=l_d=3\delta$, is actually the same. However, we note that this unstable base state does not correspond to any characteristic feature on the evolution of U_{tip}, measured in our 2D simulations. Indeed, the two remarkable events in Fig. 9 correspond to a maximum of U_{tip}, obtained at $l_t \simeq 3.5\delta$ and to the asymptotic steady state (constant U_{tip}), reached at $l_t > 5\delta$. These two states occur at l_t significantly higher than $l_d=3\delta$, which means that these 2D states are never reached in experiments, as the destabilization along the third direction y (i.e., fingering) occurs first. We recall that Goyal and Meiburg[18] performed their linear stability analysis on the 2D asymptotic steady state, and we point out that a similar analysis of the 2D base state obtained around $l_t=l_d=3\delta$ could provide enlightening results.

IV. CONCLUSIONS

We have designed an experiment to analyze, under microgravity conditions, the effect of the initial pseudointerface thickness, δ, on pure miscible viscous fingering in a Hele-Shaw cell. We have shown that the instability develops once the front has traveled a distance $l_d \sim 3\delta$, proportional to the initial thickness. On another hand, no influence of δ has been observed on the instability pattern: In particular, the selected spatial wavelength is always three times the gap thickness e, whatever the value of δ. This value differs from the value of five times the gap thickness, measured with stabilizing buoyancy,[15] but agrees with the one obtained numerically by Goyal and Meiburg,[18] in the absence of buoyancy, and for a thin initial thickness. However, these authors analyzed the stability of the steady propagating tongue, known to develop in the gap of the cell before the onset of the instability. Whereas, our experimental findings, enlightened by 2D numerical simulations of the tongue developing from a thick initial interface, support the contention that the fingering instability actually occurs before the steady state of the tongue is reached.

ACKNOWLEDGMENTS

This research was supported by the CNES and ESA, under Grant Nos. 793/CNES/00/8368 and ESA A0-99-083.We acknowledge David Charalampous, Roderick Dembet, Yann Magnin, and Jean Midy, who built the setup in the framework of "ESA Student Parabolic Flights."

[1] P. G. Saffman and G. I. Taylor, "The penetration of a fluid into a porous medium or Hele-Shaw cell containing a more viscous liquid," Proc. R. Soc. London, Ser. A **245**, 312 (1958).
[2] S. Hill, "Channeling in packed columns," Chem. Eng. Sci. **1**, 247 (1952).
[3] R. Wooding, "Growth of fingers at an unstable diffusing interface in a porous medium or Hele-Shaw cell," J. Fluid Mech. **39**, 477 (1969).
[4] G. M. Homsy, "Viscous fingering in porous media," Annu. Rev. Fluid Mech. **19**, 271 (1987).
[5] S. Tanveer, "Surprises in viscous fingering," J. Fluid Mech. **409**, 273 (2000).
[6] Z. M. Yang, Y. C. Yortsos, and D. Salin, "Asymptotic regimes in unstable miscible displacements in random porous media," Adv. Water Resour. **25**, 885 (2002).
[7] L. Paterson, "Fingering with miscible fluids in Hele-Shaw cell," Phys. Fluids **28**, 26 (1985).
[8] F. J. Manickam and G. M. Homsy, "Stability of miscible displacements in porous media with nonmonotonic viscosity profiles," Phys. Fluids A **5**, 1356 (1993).
[9] W. B. Zimmerman and G. M. Homsy, "Viscous fingering in miscible displacements: Unification of effects of viscosity contrast, anisotropic dispersion, and velocity dependence of dispersion on nonlinear propagation," Phys. Fluids A **4**, 2348 (1992).
[10] E. Lajeunesse, J. Martin, N. Rakotomalala, D. Salin, and Y. C. Yortsos, "Miscible displacement in a Hell-Shaw cell at high rates," J. Fluid Mech. **398**, 299 (1999).
[11] N. N. Smirnov, V. F. Nikitin, A. Maximenko, M. Thiercelin, and J. C. Legros, "Instability and mixing flux in frontal displacement of viscous fluids from porous media," Phys. Fluids **17**, 084102 (2005).
[12] C. T. Tan and G. M. Homsy, "Stability of miscible displacements in porous media: Rectilinear flow," Phys. Fluids **29**, 3549 (1986).
[13] G. I. Taylor, "Dispersion of soluble matter in solvent flowing slowly through a tube," Proc. R. Soc. London, Ser. A **219**, 186 (1953).
[14] N. Rakotomalala, D. Salin, and P. Watzky, "Simulations of viscous flows of complex fluids with a BGK lattice gas," Phys. Fluids **8**, 3200 (1996).
[15] E. Lajeunesse, J. Martin, N. Rakotomalala, and D. Salin, "3D instability of miscible displacements in a Hele-Shaw cell," Phys. Rev. Lett. **79**, 5254 (1997).
[16] E. Lajeunesse, J. Martin, N. Rakotomalala, D. Salin, and Y. C. Yortsos, "The threshold of the instability in miscible displacements in a Hele-Shaw cell at high rates," Phys. Fluids **13**, 799 (2001).
[17] N. Goyal, H. Pichler, and E. Meiburg, "Variable-density miscible displacements in a vertical Hele-Shaw cell: Linear stability," J. Fluid Mech. **584**, 357 (2007).
[18] N. Goyal and E. Meiburg, "Miscible displacements in Hele-Shaw cells: Two-dimensional base states and their linear stability," J. Fluid Mech. **558**, 329 (2006).
[19] Z. Yang and Y. C. Yortsos, "Asymptotic solutions of miscible displacements in geometries of large aspect ratio," Phys. Fluids **9**, 286 (1997).